BRIEF REPORT

Functional Exploration of Conserved Sequences in the Distal Face of Angiotensinogen

Naofumi Amioka[1,2,*], Chia-Hua Wu[3,*], Hisashi Sawada[1,2,4], Sohei Ito[1,2], Congqing Wu[1,2,5,6], Jessica J. Moorleghen[1,2], Deborah A. Howatt[1,2], Craig W. Vander Kooi[7], Alan Daugherty[1,2,4], Hong S. Lu[1,2,4]

[1]Saha Cardiovascular Research Center,
[2]Saha Aortic Center,
[3]Pharmacology and Nutritional Sciences,
[4]Department of Physiology,
[5]Department of Surgery,
[6]Department of Microbiology, Immunology, and Molecular Genetics
[7]Department of Molecular and Cellular Biochemistry

University of Kentucky, Lexington, KY

*These authors contributed equally to this work.

Running Title: Conserved sequences of AGT

Corresponding Authors:
Hisashi Sawada
E-mail: Hisashi.Sawada@uky.edu

Hong S. Lu
E-mail: Hong.Lu@uky.edu

Abstract:
Figures: 2
Supplemental Figures: 6
Reference: 26

ABSTRACT

Background: Angiotensinogen (AGT) is an essential component in the renin-angiotensin system. AGT has highly conserved sequences in the loop and β-sheet regions among species; however, their functions have not been studied.

Methods: Adeno-associated viral vector serotype 8 (AAV8) encoding mouse AGT with mutations of conserved sequences in the loop (AAV8.loop-Mut), β-sheet (AAV8.βsheet-Mut), or both regions (AAV8.loop/βsheet-Mut) were injected into male hepatocyte-specific AGT deficient (hepAGT-/-) mice in an LDL receptor -/- background. AAV8 containing mouse wild-type AGT (AAV8.mAGT) or a null vector (AAV8.null) were used as controls. Two weeks after AAV administration, all mice were fed Western diet for 12 weeks.

Results: In hepAGT-/- mice infected with AAV8.loop-Mut or βsheet-Mut, plasma AGT concentrations, systolic blood pressure, and atherosclerosis were comparable to those in AAV8.mAGT-infected mice. To determine the synergistic effects of conserved sequences in the loop and β-sheet regions, hepAGT-/- mice were infected with AAV8 encoding AGT with mutations in both regions. Surprisingly, plasma AGT concentrations, systolic blood pressure, and atherosclerotic lesion size in mice infected with AAV8.loop/βsheet-Mut were not different from mice infected with AAV8.null. However, hepatic *Agt* mRNA abundance was elevated to a comparable magnitude as AAV8.mAGT-infected mice. Immunostaining showed that AGT protein was accumulated in hepatocytes of mice infected with AAV8.loop/βsheet-Mut, while AGT protein was hardly detectable in hepatocytes of hepAGT-/- mice infected with AAV8.mAGT.

Conclusions: The conserved sequences in either the loop or β-sheet region individually have no effect on AGT regulation; the conserved sequences in both regions synergistically contribute to the secretion of AGT from hepatocytes.

Non-standard Abbreviations

AAV8: adeno-associated viral vector serotype 8
AGT: angiotensinogen
AngI: angiotensin I
AngII: angiotensin II
RAS: renin-angiotensin system

HIGHLIGHTS

1. The loop and β-sheet regions in the distal face of angiotensinogen (AGT) have highly conserved sequences across species.
2. Mutations on either the loop or β-sheet regions do not affect plasma AGT concentrations, blood pressure, and atherosclerosis in hypercholesterolemic mice.
3. The conserved sequences in the loop and β-sheet regions regulate the secretion of AGT from hepatocytes synergistically.

INTRODUCTION

The renin-angiotensin system (RAS) exerts crucial roles in the pathophysiology of hypertension and atherosclerosis.[1-6] Angiotensinogen (AGT), the unique substrate of the RAS, is composed of 452 amino acids in humans (453 amino acids in mice) after the cleavage of the signal peptides.[7-10] AGT is cleaved by renin to produce angiotensin I (AngI), a decapeptide that is then cleaved to produce angiotensin II (AngII, an octapeptide) and other angiotensin peptides.[9,10] Although the distal portion (the non-AngI part termed as "des(AngI)AGT") contains 98% of the amino acid of AGT, there is scant evidence regarding the role of des(AngI)AGT in regulating AngII production, AngII-mediated functions, and AngII-independent effects. des(AngI)AGT has been implicated in angiogenesis.[11,12] Our recent study supports that des(AngI)AGT contributes to diet-induced body weight gain and liver steatosis that are independent of AngII.[13,14]

In addition to the conserved AngI sequence among species, three-dimensional structure analyses identified highly conserved sequences in the loop (W292, S298, V299) and β-sheet (K253, H274, E422) regions of AGT.[10,13] These two regions are in the des(AngI)AGT portion that is far from the renin cleavage site.[13,15] A computational analysis showed that these conserved sequences are exposed to the surface of AGT. Considering their high conservation from zebrafish to humans and their locations in the AGT protein, we hypothesize that these conserved sequences have an impact on the functions of AGT.

In this study, we investigated the impact of the highly conserved sequences in the loop and β-sheet regions of AGT on the dynamics of AGT and AngII-mediated vascular functions. Since hepatocytes are the major source of AGT,[13,16-19] we used hepatocyte-specific AGT deficient (hepAGT-/-) mice. We injected adeno-associated viral vector serotype 8 (AAV8) encoding mouse AGT with mutations of conserved sequences in the loop, β-sheet, or both regions to hepAGT-/- mice. The presence of mutations in either region had no effects on AGT regulation, blood pressure, and atherosclerosis in hypercholesterolemic mice. However, mutations of the conserved sequences in both regions impacted the secretion of AGT from hepatocytes.

MATERIALS AND METHODS

Detailed materials and methods are available in the Supplemental Material.

Mice

hepAGT-/- mice and their wild-type (hepAGT+/+) littermates have been developed by breeding female *Agt* floxed mice with male albumin-Cre +/- mice as described in our previous publications.[13,16,17,20] hepAGT-/- and hepAGT+/+ littermates were generated initially in a mixed 129/C57BL/6N background and were then backcrossed to C57BL/6J strain at least 6 times.[21] All study mice were in an LDLR-/- background. Littermates were used for each experiment. Two weeks after AAV8 injections, mice were fed Western diet (Diet # TD.88137; Envigo) for 12 weeks. This study used only male mice

because of the modest response of AAV8 encoding wild-type AGT on plasma AGT concentrations in female mice.[20] All animal experiments in this study were performed according to protocols approved by the University of Kentucky Institutional Animal Care and Use Committee (IACUC protocol number 2006-0009 or 2018-2968).

Production and injection of AAV8

AAV8 was produced by the Vector Core in the Gene Therapy Program at the University of Pennsylvania. Mouse *Agt* was transduced using AAV8 that infects predominantly hepatocytes and contained a thyroxine-binding globulin (TBG) promoter for hepatocyte-specific synthesis.[22] AAV8 containing wild-type AGT (AAV8.mAGT) or an empty vector (AAV8.null) was used as controls. AAV8 ($3x10^{10}$ genome copies/mouse) were diluted in 200 µl of sterile phosphate-buffered saline (PBS) and injected into mice intraperitoneally at 6-22 weeks of age.

Systolic blood pressure measurements

Systolic blood pressure was measured at week 11 after the injection of AAV8 using a non-invasive tail-cuff system (Coda 8, Kent Scientific) following our standard protocol described previously.[23] Conscious mice were restrained in a holder and put on a heated platform. Blood pressure was measured 20 times for three consecutive days. Data showing <60 or >250 mmHg, standard deviation >30 mmHg, or successful measurements <5 cycles were excluded.

Quantification of atherosclerosis

Mice were euthanized using a ketamine/xylazine cocktail (90 and 10 mg/kg, respectively) at week 14 after the infection of AAV8. An *en face* method was used to measure atherosclerotic lesions on the intimal surface of the thoracic aorta, as described previously.[24,25] The aorta was dissected and fixed in 10% neutrally buffered formalin overnight. Subsequently, perivascular tissues were removed and the intimal surface was exposed by a longitudinal cut. Aortas were then pinned on a black wax surface and *en face* images were captured using a digital camera (DS-Ri1, Nikon). All image processing and analyses were performed using a Nikon NIS-Elements software (NIS-Elements AR 5.11.0.) Atherosclerotic lesions were traced manually on the *en face* images from the ascending aorta to 3 mm distal from the orifice of the left subclavian artery. Measured data were verified independently by an investigator who was blinded to the study groups. Atherosclerotic lesion size was presented as percent lesion area as below:

$$\text{Percent lesion area} = \frac{\text{Atherosclerotic lesion (mm}^2\text{)}}{\text{Intimal area of the aorta (mm}^2\text{)}} \times 100$$

Statistical analysis

SigmaPlot version 14.5 or 15 (SYSTAT Software Inc.) was used for graphs and statistical analyses. Data are presented as the median and 25th/75th percentiles. Kruskal-Wallis one-way ANOVA on ranks followed by Dunn's method was used for statistical analysis. $P<0.05$ was considered statistically significant.

RESULTS

AAV8-driven expression of wild-type AGT increased plasma AGT concentrations and vascular functions in hepAGT-/- mice.
We first confirmed the effects of AAV8 encoding wild-type mouse AGT on plasma AGT concentrations, systolic blood pressure and atherosclerosis in hepAGT-/- mice. Infection of AAV8.mAGT increased plasma AGT concentrations in hepAGT-/- mice that were comparable to the plasma AGT concentrations in hepAGT+/+ littermates infected with AAV8 containing an empty vector (**Supplemental Figure 1A**). Systolic blood pressure and atherosclerotic lesion area were increased by AAV8.mAGT infection in hepAGT-/- mice to the same magnitude as in their hepAGT+/+ littermates infected with AAV8.null. Plasma total cholesterol concentrations were not different among hepAGT+/+ mice infected with AAV8.null, hepAGT-/- mice infected with AAV8.null, and hepAGT-/- mice infected with AAV8.mAGT (**Supplemental Figure 1B-D**). Therefore, in the subsequent studies, we used AAV8.mAGT infection in hepAGT-/- mice to represent its wild-type control (hepAGT+/+).

Mutations of conserved sequences in either the loop or β-sheet region of AGT increased plasma AGT concentrations and vascular functions in hepAGT-/- mice.
Computational analyses revealed highly conserved sequences in the two distal face regions, the loop and β-sheet regions, of AGT (**Figure 1A**). We first determined roles of the conserved sequences in the loop region on plasma AGT concentrations, systolic blood pressure regulation and atherosclerosis. Genetic manipulation was conducted by replacing the three conserved residues in the loop region (W292, S298, V299) with alanine (**Figure 1B**). AAV8 encoding AGT with these mutations (AAV8.loop-Mut) was injected into hepAGT-/- mice. Two weeks after the AAV injections, AAV8.loop-Mut increased plasma AGT concentrations significantly in hepAGT-/- mice, which were comparable to those in hepAGT-/- mice infected with AAV8.mAGT (**Figure 1C**). Plasma renin concentrations (PRC) were suppressed equivalently by the population of loop-Mut and mouse wild-type AGT (**Supplemental Figure 2A**). In comparisons with hepAGT-/- mice infected with AAV8.null, infection of AAV8.loop-Mut increased systolic blood pressure and atherosclerotic lesions. These phenotypes were not different from hepAGT-/- mice infected with AAV8.mAGT (**Figure 1D, 1E**). Plasma total cholesterol concentrations were modestly higher in AAV8.loop-Mut and AAV8.mAGT-AAV infected mice, compared to AAV8.null-infected mice (**Supplemental Figure 2B**).

We next determined functions of the highly conserved sequences in the β-sheet region on plasma AGT concentrations and vascular functions. The 3 highly conserved amino acid residues (K253, H274, E422) of the β-sheet region were replaced by alanine (**Figure 1F**), and AAV8 with mutations of these 3 residues (AAV8.βsheet-Mut) were injected into hepAGT-/- mice. Injection of AAV8.βsheet-Mut increased plasma AGT concentrations similar to mice injected with AAV8.mAGT (**Figure 1G**). Population of βsheet-Mut also increased systolic blood pressure and atherosclerosis lesions in hepAGT-/- mice (**Figure 1H, I**). PRC was suppressed equivalently by AAV8.βsheet-Mut and AAV8.mAGT (**Supplemental Figure 3A**). Plasma total cholesterol concentrations were not different among the 3 groups (**Supplemental Figure 3B**).

Mutations of the conserved residues in both the loop and β-sheet regions did not change plasma AGT concentrations and vascular functions in hepAGT-/- mice. We next generated AAV8 encoding mouse AGT with mutations on the conserved amino acid residues of both the loop and β-sheet regions (AAV8.loop/βsheet-Mut). The computational analysis did not detect major structural changes by the mutations. Unlike AGT with mutations in either region, plasma AGT concentrations were not increased (**Figure 2A**) and PRC was not altered (**Supplemental Figure 4A**) by AAV8.loop/βsheet-Mut infection in hepAGT-/- mice. Plasma total cholesterol concentrations did not differ among the 3 groups (**Supplemental Figure 4B**). AAV8.loop/βsheet-Mut did not increase systolic blood pressure or augment atherosclerotic lesion size (**Figure 2B and C**). These results suggest that the conserved sequences in the loop and β-sheet regions have synergistic effects on plasma AGT concentrations and vascular functions.

Liver is the primary source for AGT production,[13,16-18] and the AAVs we used predominantly populates AGT in hepatocytes.[22] Therefore, we examined the abundance of hepatic *Agt* mRNA by qPCR. Hepatic *Agt* mRNA was comparable between mice infected with AAV8.loop/βsheet-Mut and AAV8.mAGT (**Figure 2D**). A previous study reported that AAV8 predominantly leads to infection in pericentral hepatocytes.[22] Consistently, in situ hybridization by RNAscope revealed the presence of *Agt* mRNA in hepatocytes, predominantly in pericentral hepatocytes of both AAV8.loop/βsheet-Mut- and AAV8.mAGT-infected mice, but not in AAV8.null-infected mice (**Figure 2E**). We have not been able to detect AGT protein in hepatocytes in hepAGT+/+ mice under normal conditions using immunostaining, although it has been found consistently in renal proximal tubule cells (**Supplemental Figure 5A and B**). As expected, AGT protein was not detected in hepatocytes of AAV8.mAGT-infected mice (**Figure 2F**). However, AGT protein was accumulated in hepatocytes of mice infected with AAV8.loop/βsheet-Mut, as detected by immunostaining (**Figure 2F**). Accumulation of AGT protein was predominantly in pericentral hepatocytes as confirmed with immunostaining of glutamine synthetase, an enzyme that is abundant in hepatocytes surrounding central veins (**Supplemental Figure 6A and B**).

DISCUSSION

Our study is the first to determine whether the highly conserved sequences in the distal regions of AGT are functionally important for AGT regulation. We used mice in which the *Agt* gene was deleted specifically in hepatocytes. Mouse AGT containing mutations of the conserved residues in the loop, β-sheet, or both regions were populated to the liver of this mouse model by an AAV vector. This AAV serotype 8 vector containing the TBG promoter targets hepatocytes with high specificity.[22,26] We used AAV8 containing a null vector as a negative control and AAV8 containing wild-type mouse AGT as a positive control. We have demonstrated consistently in this and previous studies that the genome copies of AAV8 encoding mouse wild-type AGT in hepAGT-/- mice led to comparable plasma AGT concentrations and AngII-mediated vascular functions such as blood pressure and atherosclerosis with those in hepAGT+/+ mice.[13,16,20] Comparable to

hepAGT-/- mice infected with AAV8.mAGT, plasma AGT concentrations were increased in hepAGT-/- mice infected with AAV8.loop-Mut or AAV.βsheet-Mut alone, but not in hepAGT-/- mice infected with AAV8.loop/βsheet-Mut. It is surprising that mutations of conserved sequences in either region did not affect AGT regulation and AGT-mediated vascular functions, while the conserved sequences of both regions in combination are needed to maintain the normal regulation of AGT. Overall, these data suggest that the des(AngI)AGT part of AGT has modest effects on AGT regulation.

mRNA abundance of AGT in liver of hepAGT-/- mice infected with AAV8.loop/βsheet-Mut was equivalent to its abundance in liver of hepAGT-/- mice infected with AAV8.mAGT, supporting that the mutations of the conserved sequences do not affect AGT mRNA expression. Under normal conditions, AGT is produced and secreted rapidly from hepatocytes to plasma. Therefore, it is technically difficult to detect AGT protein in hepatocytes by immunostaining. In contrast, we found that high abundance of AGT protein, as demonstrated by immunostaining, was accumulated in hepatocytes surrounding central veins in liver sections of hepAGT-/- mice infected with AAV8.loop/βsheet-Mut. These findings implicate that the conserved sequences in the β-sheet and loop regions of AGT do not affect mRNA or protein production, but impair the secretion of AGT protein from hepatopcytes. Consequently, plasma AGT concentration remained low, and systolic blood pressure and atherosclerosis were not changed in hepAGT-/- mice infected with AAV8.loop/βsheet-Mut. The mechanism by which this occurs is unclear. Although the computational analysis did not support the notion that mutations of the conserved sequences in both regions affect the AGT structure, this has not been able to be confirmed using an in vivo technique.

In contrast to the modest effects on AGT regulation, our recent studies support that des(AngI)AGT, containing 442 amino acids, has a pathophysiological function.[13] hepAGT-/- mice have less body weight gain and improved liver steatosis when fed Western diet, compared to their wild-type littermates.[13,14] The induction of the des(AngI)AGT portion of mouse AGT into hepatocytes of hepAGT-/- mice using the same AAV8 approach replenished Western diet-induced body weight gain and liver steatosis, supporting that des(AngI)AGT itself regulates metabolism. Mutations of the conserved sequences in either the loop or the β-sheet region did not affect body weight gain, implicating that neither region affects des(AngI)AGT function alone. However, the present study is not able to conclude whether both conserved sequences are required to maintain des(AngI)AGT function on body weight and steatosis due to the impaired secretion of the AGT protein.

In conclusion, the present study provides evidence that the conserved sequences from the loop and β-sheet regions of AGT in combination contribute to AGT protein secretion from hepatocytes in mice.

Sources of Funding

This research work is supported by the National Heart, Lung, and Blood Institute of the National Institutes of Health (R01HL139748). The content in this article is solely the responsibility of the authors and does not necessarily represent the official views of the

National Institutes of Health.

Disclosure

None.

REFERENCES

1. Daugherty A, Manning MW, Cassis LA. Angiotensin II promotes atherosclerotic lesions and aneurysms in apolipoprotein E-deficient mice. *J Clin Invest*. 2000;105:1605-1612. doi: 10.1172/jci7818
2. Ruiz-Ortega M, Lorenzo O, Rupérez M, Esteban V, Suzuki Y, Mezzano S, Plaza JJ, Egido J. Role of the renin-angiotensin system in vascular diseases: expanding the field. *Hypertension*. 2001;38:1382-1387. doi: 10.1161/hy1201.100589
3. Weiss D, Sorescu D, Taylor WR. Angiotensin II and atherosclerosis. *Am J Cardiol*. 2001;87:25c-32c. doi: 10.1016/s0002-9149(01)01539-9
4. Weiss D, Kools JJ, Taylor WR. Angiotensin II-induced hypertension accelerates the development of atherosclerosis in apoE-deficient mice. *Circulation*. 2001;103:448-454. doi: 10.1161/01.cir.103.3.448
5. Rajagopalan S, Kurz S, Münzel T, Tarpey M, Freeman BA, Griendling KK, Harrison DG. Angiotensin II-mediated hypertension in the rat increases vascular superoxide production via membrane NADH/NADPH oxidase activation. Contribution to alterations of vasomotor tone. *J Clin Invest*. 1996;97:1916-1923. doi: 10.1172/jci118623
6. Mehta PK, Griendling KK. Angiotensin II cell signaling: physiological and pathological effects in the cardiovascular system. *Am J Physiol Cell Physiol*. 2007;292:C82-97. doi: 10.1152/ajpcell.00287.2006
7. Clouston WM, Evans BA, Haralambidis J, Richards RI. Molecular cloning of the mouse angiotensinogen gene. *Genomics*. 1988;2:240-248. doi: 10.1016/0888-7543(88)90008-0
8. Lynch KR, Peach MJ. Molecular biology of angiotensinogen. *Hypertension*. 1991;17:263-269. doi: 10.1161/01.hyp.17.3.263
9. Wu C, Lu H, Cassis LA, Daugherty A. Molecular and pathophysiological features of angiotensinogen: A mini review. *N Am J Med Sci (Boston)*. 2011;4:183-190. doi: 10.7156/v4i4p183
10. Lu H, Cassis LA, Kooi CW, Daugherty A. Structure and functions of angiotensinogen. *Hypertens Res*. 2016;39:492-500. doi: 10.1038/hr.2016.17
11. Célérier J, Cruz A, Lamandé N, Gasc JM, Corvol P. Angiotensinogen and its cleaved derivatives inhibit angiogenesis. *Hypertension*. 2002;39:224-228. doi: 10.1161/hy0202.103441
12. Corvol P, Lamandé N, Cruz A, Celerier J, Gasc JM. Inhibition of angiogenesis: a new function for angiotensinogen and des(angiotensin I)angiotensinogen. *Curr Hypertens Rep*. 2003;5:149-154. doi: 10.1007/s11906-003-0072-3
13. Lu H, Wu C, Howatt DA, Balakrishnan A, Moorleghen JJ, Chen X, Zhao M, Graham MJ, Mullick AE, Crooke RM, et al. Angiotensinogen exerts effects independent of angiotensin II. *Arterioscler Thromb Vasc Biol*. 2016;36:256-265.

doi: 10.1161/atvbaha.115.306740
14. Tao XR, Rong JB, Lu HS, Daugherty A, Shi P, Ke CL, Zhang ZC, Xu YC, Wang JA. Angiotensinogen in hepatocytes contributes to Western diet-induced liver steatosis. *J Lipid Res*. 2019;60:1983-1995. doi: 10.1194/jlr.M093252
15. Zhou A, Carrell RW, Murphy MP, Wei Z, Yan Y, Stanley PL, Stein PE, Broughton Pipkin F, Read RJ. A redox switch in angiotensinogen modulates angiotensin release. *Nature*. 2010;468:108-111. doi: 10.1038/nature09505
16. Wu C, Xu Y, Lu H, Howatt DA, Balakrishnan A, Moorleghen JJ, Vander Kooi CW, Cassis LA, Wang JA, Daugherty A. Cys18-Cys137 disulfide bond in mouse angiotensinogen does not affect AngII-dependent functions in vivo. *Hypertension*. 2015;65:800-805. doi: 10.1161/hypertensionaha.115.05166
17. Ye F, Wang Y, Wu C, Howatt DA, Wu CH, Balakrishnan A, Mullick AE, Graham MJ, Danser AHJ, Wang J, et al. Angiotensinogen and megalin interactions contribute to atherosclerosis-Brief report. *Arterioscler Thromb Vasc Biol*. 2019;39:150-155. doi: 10.1161/atvbaha.118.311817
18. Matsusaka T, Niimura F, Shimizu A, Pastan I, Saito A, Kobori H, Nishiyama A, Ichikawa I. Liver angiotensinogen is the primary source of renal angiotensin II. *J Am Soc Nephrol*. 2012;23:1181-1189. doi: 10.1681/asn.2011121159
19. Yiannikouris F, Wang Y, Shoemaker R, Larian N, Thompson J, English VL, Charnigo R, Su W, Gong M, Cassis LA. Deficiency of angiotensinogen in hepatocytes markedly decreases blood pressure in lean and obese male mice. *Hypertension*. 2015;66:836-842. doi: 10.1161/hypertensionaha.115.06040
20. Wu CH, Wu C, Howatt DA, Moorleghen JJ, Cassis LA, Daugherty A, Lu HS. Two Amino Acids Proximate to the Renin Cleavage Site of Human Angiotensinogen Do Not Affect Blood Pressure and Atherosclerosis in Mice-Brief Report. *Arterioscler Thromb Vasc Biol*. 2020;40:2108-2113. doi: 10.1161/atvbaha.120.314048
21. Ye D, Wu C, Chen H, Liang CL, Howatt DA, Franklin MK, Moorleghen JJ, Tyagi SC, Uijl E, Danser AHJ, et al. Fludrocortisone induces aortic pathologies in mice. *Biomolecules*. 2022;12. doi: 10.3390/biom12060825
22. Bell P, Wang L, Gao G, Haskins ME, Tarantal AF, McCarter RJ, Zhu Y, Yu H, Wilson JM. Inverse zonation of hepatocyte transduction with AAV vectors between mice and non-human primates. *Mol Genet Metab*. 2011;104:395-403. doi: 10.1016/j.ymgme.2011.06.002
23. Daugherty A, Rateri D, Hong L, Balakrishnan A. Measuring blood pressure in mice using volume pressure recording, a tail-cuff method. *J Vis Exp*. 2009. doi: 10.3791/1291
24. Daugherty A, Tall AR, Daemen M, Falk E, Fisher EA, García-Cardeña G, Lusis AJ, Owens AP, 3rd, Rosenfeld ME, Virmani R. Recommendation on design, execution, and reporting of animal atherosclerosis studies: A scientific statement from the American Heart Association. *Arterioscler Thromb Vasc Biol*. 2017;37:e131-e157. doi: 10.1161/atv.0000000000000062
25. Chen H, Howatt DA, Franklin MK, Amioka N, Sawada H, Daugherty A, Lu HS. A mini-review on quantification of atherosclerosis in hypercholesterolemic mice. *Global Translational Medicine*. 2022;1:76. doi: 10.36922/gtm.v1i1.76
26. Chen SJ, Sanmiguel J, Lock M, McMenamin D, Draper C, Limberis MP, Kassim

SH, Somanathan S, Bell P, Johnston JC, et al. Biodistribution of AAV8 vectors expressing human low-density lipoprotein receptor in a mouse model of homozygous familial hypercholesterolemia. *Hum Gene Ther Clin Dev*. 2013;24:154-160. doi: 10.1089/humc.2013.082

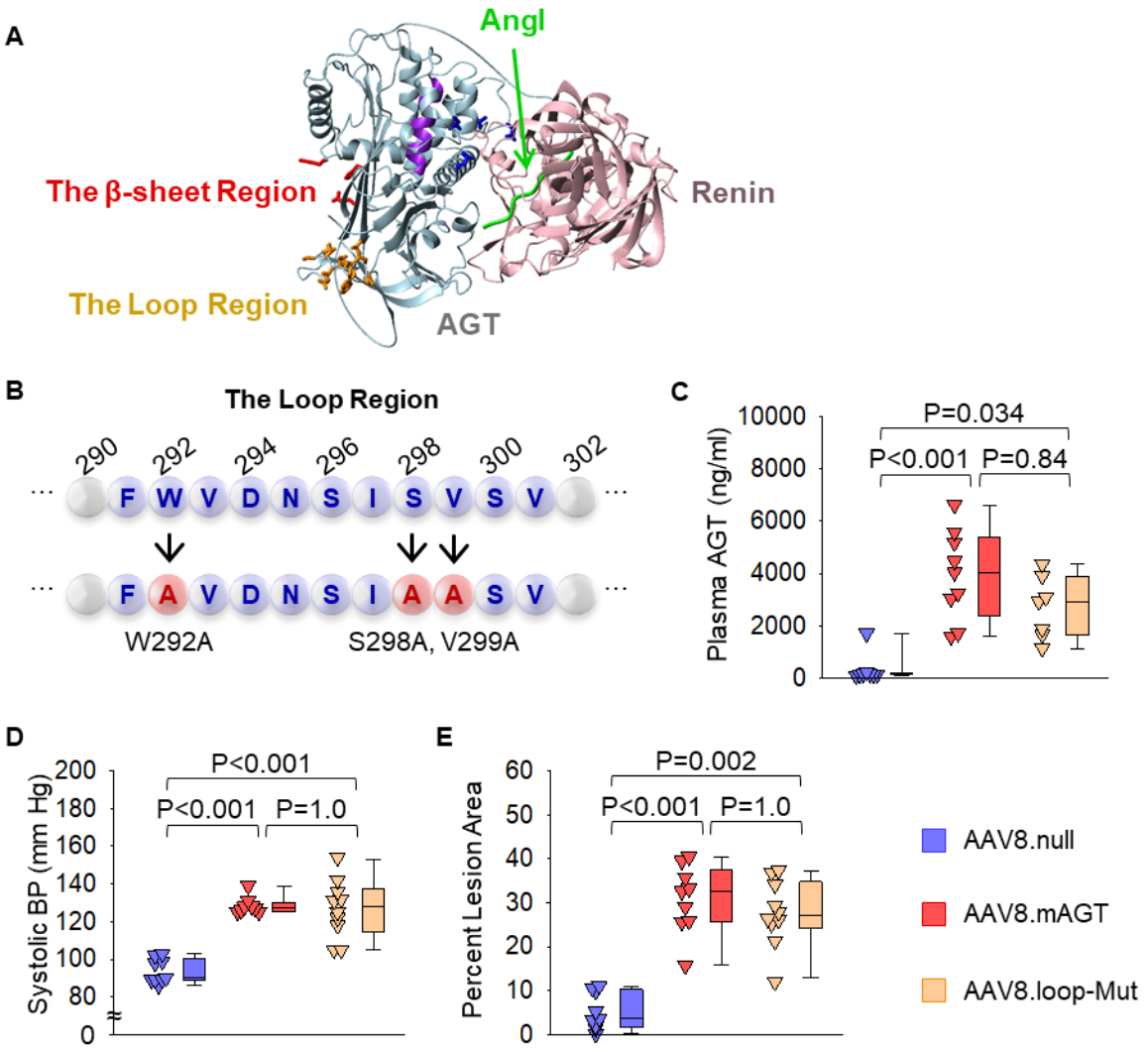

Figure 1. Mutations of conserved residues in either the loop or β-sheet region of AGT had comparable effects as wild-type AGT on plasma AGT concentrations, blood pressure, and atherosclerosis in hepAGT-/- mice. (A) Computational analysis for the three-dimensional structure of AGT and renin. The distal surface is highlighted in gold for the loop region and red for the β-sheet region. Green represents angiotensin I (AngI). **(B)** The 3 amino acid residues identical across species were replaced with alanine in the loop (W292A, S298A, V299A). **(C-E)** Male hepAGT -/- mice infected with AAV8 were fed Western diet for 12 weeks. **(C)** Plasma AGT concentrations, **(D)** systolic blood pressures (BP), and **(E)** percent lesion area of atherosclerosis in hepAGT-/- mice (n = 7-10 per group) infected with AAV8.null, AAV8.mAGT, or AAV8 encoding AGT with mutations in the loop region (AAV8.loop-Mut). P values were determined by Kruskal-Wallis one-way ANOVA on Ranks followed by Dunn's test. **(Figure continues on next page)**

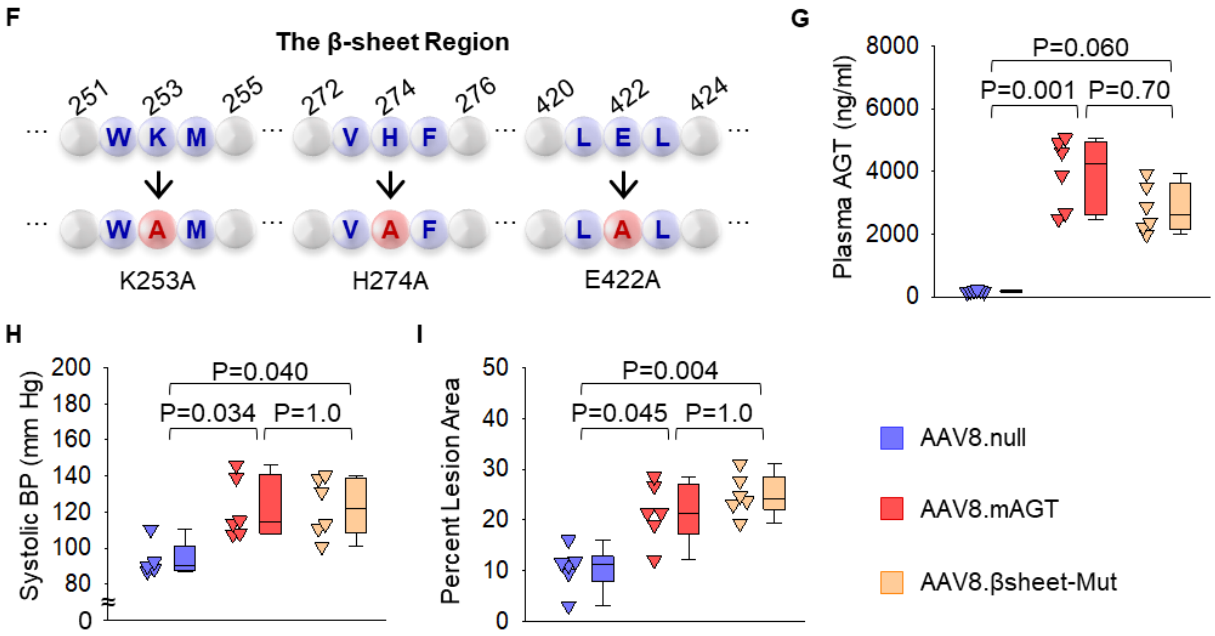

Figure 1. (continued) (F) The 3 amino acid residues identical across species were replaced with alanine in the β-sheet (K253A, H274A, E422A) regions. **(G-I)** Male hepAGT -/- mice infected with AAV8 were fed Western diet for 12 weeks. **(G)** Plasma AGT concentrations, **(H)** systolic blood pressures (BP), and **(I)** percent lesion area of atherosclerosis in hepAGT-/- mice (n = 5-6 mice per group) infected with AAV8.null, AAV8.mAGT, or AAV8 encoding AGT with mutations in the β-sheet region (AAV8.βsheet-Mut). P values were determined by Kruskal-Wallis one-way ANOVA on Ranks followed by Dunn's test.

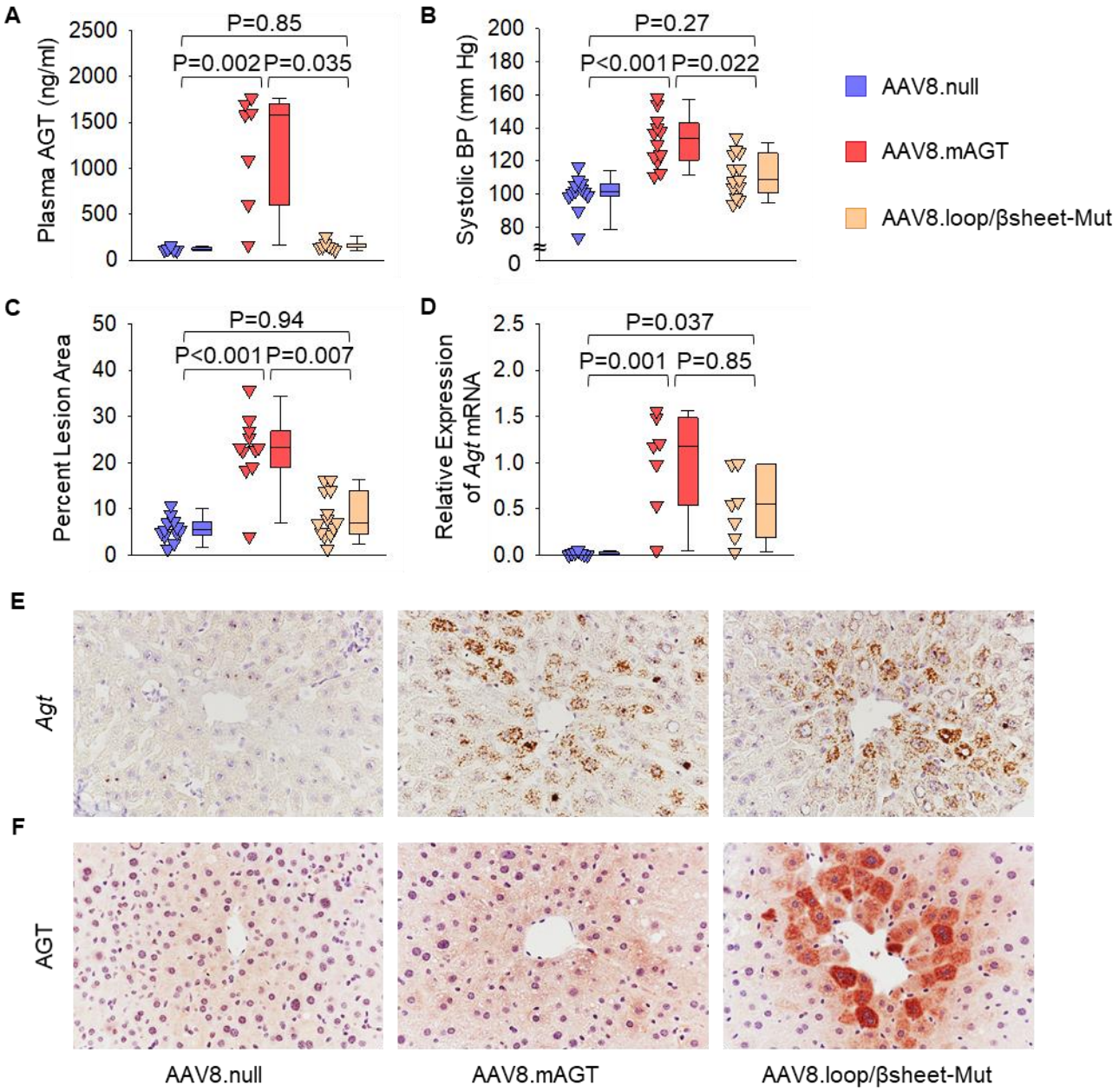

Figure 2. Mutations of conserved residues in both the loop and β-sheet regions of AGT did not increase plasma AGT concentrations, blood pressure, or atherosclerosis in hepatocyte-specific AGT deficient mice. (A) Plasma AGT concentrations, **(B)** systolic blood pressures (BP), **(C)** percent lesion area of atherosclerosis, **(D)** *Agt* mRNA abundance in liver, **(E)** RNAscope of *Agt* mRNA in liver, and **(F)** immunostaining of AGT in liver of hepAGT-/- mice infected with AAV8.null, AAV8.mAGT, or AAV8.loop/βsheet-Mut (n = 5-13 per group). P values were determined by Kruskal-Wallis one-way ANOVA on Ranks followed by Dunn's test.